RSC Advances

ROYAL SOCIETY
OF CHEMISTRY

www.rsc.org/advances

Designing 3D graphene networks via 3D-printed Ni template

Zhuxian Yang [a], Chunze Yan [a], Jinhui Liu [b], Sakineh Chabi [a], Yongde Xia [a] and Yanqiu Zhu [a*]

[a] College of Engineering, Mathematics and Physical Sciences, University of Exeter, Exeter EX4 4QF, United Kingdom. *Tel: 44 1392 723620; E-mail: y.zhu@exeter.ac.uk*

[b] Modern manufacture engineering centre, Heilongjiang Institute of Science and Technology, Heilongjiang 150022, China

Abstract

It is highly desirable to design and control the 3D graphene networks with preferred shapes, lengths, diameters of the trusses so as to add new functionalities. Hereby, we demonstrate a conceptual design and practical synthesis of periodic 3D graphene networks via CVD using a 3D-printed Ni scaffold as the template.

Since the first isolation of single layer closely packed two-dimensional (2D) honeycomb structures by a mechanical cleavage of graphite in 2004 [1], graphene has been demonstrated with many exceptional properties, including outstanding electron mobility, excellent thermal conductivity, extremely high mechanical strength, high optical transparency, and large theoretical specific surface area. However, in order to harness those properties, it is necessary to integrate individual 2D graphene sheets into macrostructures for macroscopic applications. Recently, the preparation of freestanding 3D graphene foams by chemical vapor deposition (CVD) has opened a way to explore graphene [2, 3], because these 3D graphene foams can offer high electrical conductivity and improved structural stability, due to the absence of defects and intersheet junction contact resistance, compared to those graphene-based thin film composites and freestanding nanosheets [4].

However, in the 3D graphene foams, either produced by Ni-templated growth or by the sugar blowing technique without any template, their pore shapes and geometries are arranged randomly. To maximise the potentials for their applications, it is intriguing to introduce a controllable

---

[*] Corresponding author. E-mail: y.zhu@exeter.ac.uk (Yanqiu Zhu)

element into the 3D structures, which are expected to produce additional new functionalities. To create such designed 3D graphene architectures is therefore the main research objectives of this report. We will demonstrate for the first time the production of a conceptually designed 3D graphene networks via 3D-printed Ni-templated chemical vapour deposition (CVD) at 1000°C using styrene as the carbon source. Detailed synthesis and characterisations are given in supporting information.

The SEM images of as-received 3D-printed Ni templates are shown in Figure 1 (A, B). For easy comparison, the surface of random 3D Ni foam (1.6 mm thick, kindly provided by Novamet, USA) is presented in Figure 1D. Produced from a chemical process, the truss surface of the random Ni foam appears smooth and clean, with visible grain boundaries for the Ni. In contrast, Figure 1A shows that the designed Ni template is very well arranged, with strut length around 1 mm. However, the surface of the template appears very rough, covered with agglomerated particles of various sizes, without any observable grain boundaries, and the templates were very brittle. This is probably due to the unoptimised printing parameters which led to poorly sintered particles. It has been reported that the surface smoothness and grain size of the Ni template play an important role in producing high quality large area graphene via CVD. Usually an annealing process is carried out to clean and smoothen the surface, and to increase the grain size of the Ni substrate before the CVD process [5]. After annealing at 1370°C (below its melting point of 1455°C) for 9 h under Ar and H_2, the surface became smoother and cleaner (almost free of the previously agglomerated particles), and the grain boundaries of Ni were clearly shown (Figure 1C); meanwhile, structurally the template became very robust. This indicates that the annealing process has improved the crystalisation and mechanical strength of the 3D-printed Ni scaffold, making it suitable as a template for the following graphene growth step. It is worth pointing out that a better quality 3D-printed Ni scaffold may not need this annealing process, but for the studied preliminary samples, it is a very useful step to obtain larger grains for better quality graphene growth. The annealed Ni templates were further characterised by Micro-CT. As shown in Figure 1 (E, F), the Micro-CT results are in good agreement with the SEM results that the template is very well arranged.

The SEM images of the graphene/Ni networks are presented in Figure 2 (A, B). The presence of wrinkles in the images is a typical characteristic for graphene, indicating the successful deposition of graphene on the 3D-printed Ni template. It is generally accepted that the origin of the

wrinkles is due to the difference between the thermal expansion coefficients of the Ni substrate and the graphene layers [6]. Figure 2 (C, D and E) presents the HRTEM images of the graphene flakes falling off the graphene/Ni composite networks due to the powerful ultrasonic probe treatment during the TEM sample preparation. Based on many observations, the estimated layer number of the graphene in this case is around 8 (it is worth noting that this value might be under estimated due to the sonication process which may lead to the graphene flake exfoliation), which is comparable with the results we obtained on the random Ni foam under similar CVD conditions. The inset in Figure 2E is the electron diffraction pattern taken from a very thin nanosheet lying flat on the grid surface. The two typical rings of produced by the (100) and (110) planes are visible, indicating the polycrystalline feature of the graphene. To further confirm the growth of graphene and evaluate its quality, Raman spectra were recorded. The Raman spectra shown in Figure 3F were measured at three random positions to check the homogeneity of the sample. There are three peaks visible: the D peak (~ 1350 cm^{-1}) due to defects; the G peak (~ 1580 cm^{-1}) assigned to the bond stretching of the pairs of sp^2 graphitic carbon atom; and the 2D peak (~ 2680 cm^{-1}) corresponding to the high-energy second-order process. The appearance of the G peak around 1580 cm^{-1} and the 2D peak around 2720 cm^{-1}, together with the SEM and TEM images, further confirms the presence of graphene. Considering the intensity of the G and 2D peaks with a pretty much consistent ratio of $I_G/I_{2D} \sim 2.4$, we conclude the graphene is multilayer [7], which again is in good agreement with the above TEM observation. In addition, the intensity ratio of the I_D/I_G is less than 0.1, which is much lower than the reported I_D/I_G value of 0.45 for the 4-layer mechanically cleavage graphene [8], confirming the good integrity of the resulting graphene in the 3D foam.
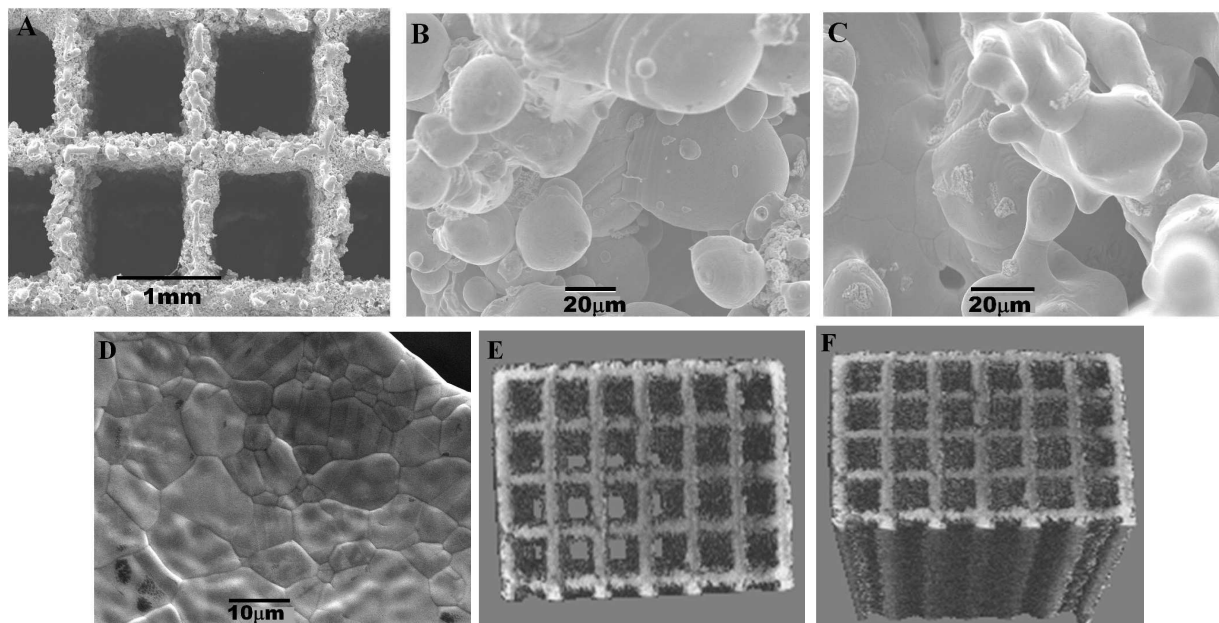
Fig. 1 SEM images of the as-received 3D-printed Ni scaffold before (A, B) and after (C) annealing at 1370°C and the as-received random Ni foam (D); Micro-CT images of the 3D-printed Ni scaffold after annealing at 1370°C (E, F)
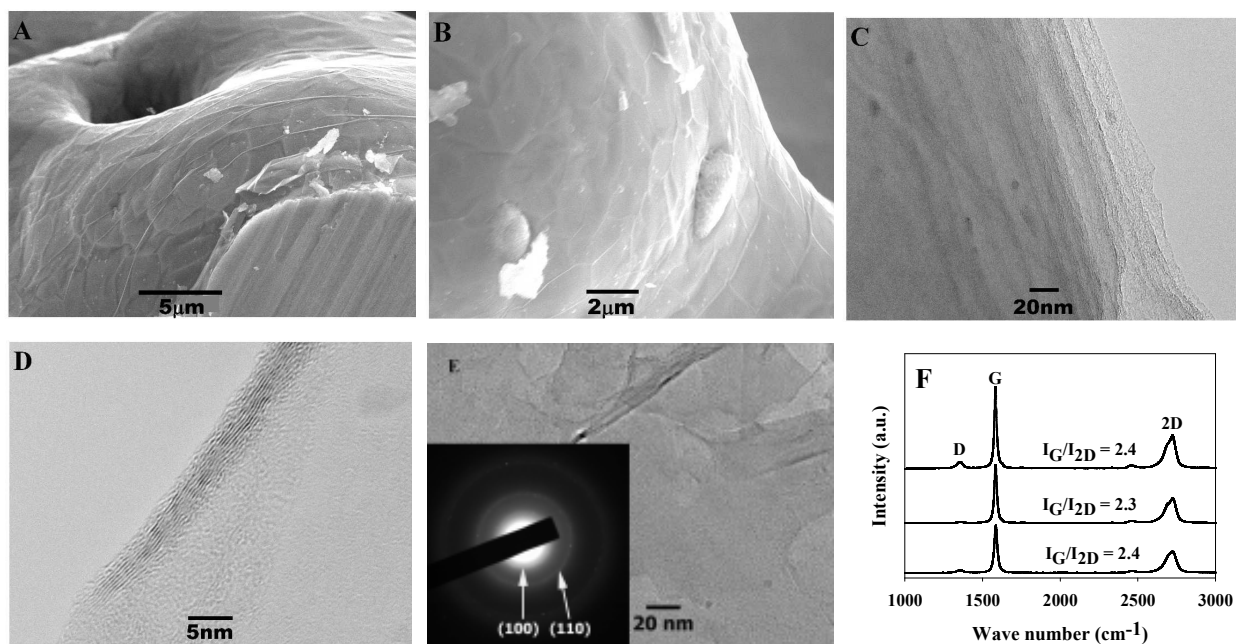
Fig. 2 SEM images (A, B), TEM images (C, D, E) and Raman shifts (F) of the as-grown graphene on a 3D-printed Ni template

4

In order to obtain 3D graphene networks, the resulting 3D-printed Ni/graphene composite was refluxed in 3 M HCl at 80 °C to remove the Ni template. The refluxed sample was subsequently characterised using EDS (Figures 1S and 2S). The result shows that only a trace amount of Ni is detected, indicating the successful removal of the Ni template. The SEM images of the 3D graphene networks are presented in Figure 3. Compared with Figure 1A, Figure 3A clearly shows that the graphene has retained the networks of the 3D-printed Ni template except that the framework is not as rigid as the Ni template, as evidenced by the bent trusses. Figure 3 (B, C) show the SEM images with higher magnification. The broken graphene (Figure 3B) was originated from the rapid etching process at high temperature (80°C), in which the escape of H_2 upon pressure building up broke some weak defective layers. However, coating a PMMA layer to protect the graphene before HCl refluxing produced only slightly improved results. The winkles that are typical for graphene can be easily observed in Figure 3C, further confirming the successful etching process that preserved the 3D network structures. It is worth noting that this 3D structure is templated with the very preliminary 3D-printed Ni scaffold, so it is no doubt that rigid 3D graphene networks can be achieved by using an optimised 3D printed Ni template. Based on the EDS, SEM, TEM and Raman results, it can be concluded that 3D graphene networks templated from the 3D-printed Ni scaffold has been successfully prepared. It is worth pointing out that the unit cell of this CVD templated 3D graphene networks is in millimeter scale, differing from the reported 3D periodic porous graphene networks having pore sizes around 500 nm (in nanoscale) which was chemically converted from amorphous porous carbon [9]. Compared with the random Ni foam as templates, in which the pore shapes and geometries of the resulting 3D graphene foam networks are arbitrarily arranged, the advantage of using 3D-printed Ni scaffolds as the template is that it can be controlled to provide desired shapes, lengths, diameters and contact angles of the trusses etc., which will offer additional new functionalities for the resulting 3D graphene networks, so as to widen the applications well beyond those randomly arranged 3D graphene foam networks, in terms of structural stability, porosity and mechanical strength etc.
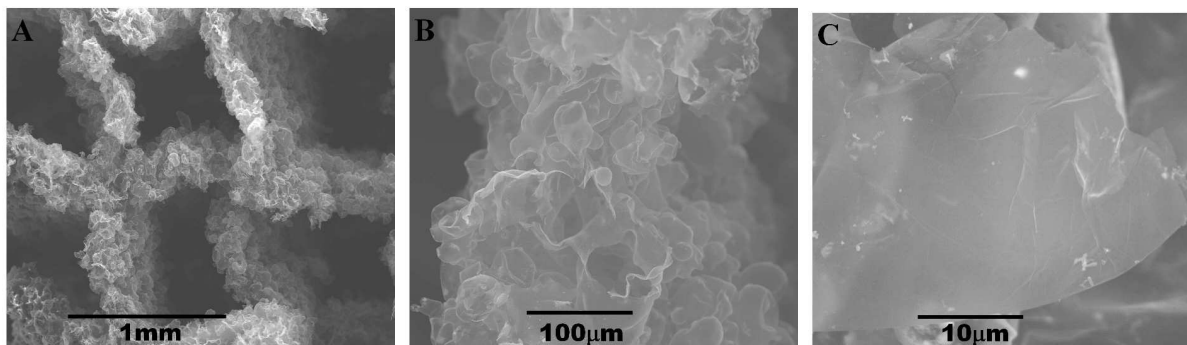
Fig. 3 SEM images of 3D graphene networks at various magnifications: 1 mm (A), 100 μm (B) and 10 μm (C)

The creation of a conceptually designed 3D graphene networks via 3D-printed Ni-templated CVD demonstrated in this report shows only very simple 3D structures and other model of 3D-printed Ni templates are under study, however this could be a step change for much complex 3D graphene networks applications. Indeed 3D printing as a technique is still at its infancy, but with huge potential. The designing of functional template structures with various configurations is only a matter of technical issue. The recent development on 3D printing techniques for porous structures with super-high resolution down to 10 nm, such as the 2PP technique [10], shed further light on the ultra-fine template design and production. Accordingly, by taking advantage of the full potential of 3D printing for Ni or Cu template creation and the versatile feature of the CVD process for graphene growth, we believe that customised 3D graphene networks with tuneable trusses and features can be further produced to suit for specific requirements ideal for applications in acoustic and optical, electromagnetic, photonic and mechanical field.

Conclusions

We report the first successful design and the generation of a 3D graphene networks using a 3D-printed Ni template and a CVD process at 1000°C. The as-grown 3D Ni/graphene composite networks or the template-free 3D graphene network have been characterised using Raman, EDS, SEM and TEM, and the results show that the graphene is of very good quality, with around 8 graphene layers. Due to the combination of the 3D periodic structure and the outstanding properties of graphene, plus the wide adjustability of the truss type and geometries, such 3D

graphene networks are expected to be attractive in acoustic and optical, electromagnetic and photonic applications.

Acknowledgement

References

1.   K. S. Novoselov, A. K. Geim, S. V. Morozov, D. Jiang, Y. Zhang, S. V. Dubonos, I. V. Grigorieva and A. A. Firsov, *Science*, 2004, **306**, 666.
2.   Z. P. Chen, W. C. Ren, L. B. Gao, B. L. Liu, S. F. Pei and H. M. Cheng, *Nature Materials*, 2011, **10**, 424.
3.   X. H. Cao, Y. M. Shi, W. H. Shi, G. Lu, X. Huang, Q. Y. Yan, Q. C. Zhang and H. Zhang, *Small*, 2011, **7**, 3163.
4.   M. D. Stoller, S. J. Park, Y. W. Zhu, J. H. An and R. S. Ruoff, *Nano Lett.*, 2008, **8**, 3498.
5.   S. Thiele, A. Reina, P. Healey, J. Kedzierski, P. Wyatt, P.-L. Hsu, C. Keast, J. Schaefer and J. Kong, *Nanotechnology*, 2010, **21**(1):015601.
6.   S. J. Chae, F. Gunes, K. K. Kim, E. S. Kim, G. H. Han, S. M. Kim, H. J. Shin, S. M. Yoon, J. Y. Choi, M. H. Park, C. W. Yang, D. Pribat and Y. H. Lee, *Adv. Mater.*, 2009, **21**, 2328.
7.   A. C. Ferrari, J. C. Meyer, V. Scardaci, C. Casiraghi, M. Lazzeri, F. Mauri, S. Piscanec, D. Jiang, K. S. Novoselov, S. Roth and A. K. Geim, *Phys. Rev. Lett.*, 2006, **97**, 4.
8.   I. Janowska, F. Vigneron, D. Begin, O. Ersen, P. Bernhardt, T. Romero, M. J. Ledoux and C. Pham-Huu, *Carbon*, 2012, **50**, 3106.
9.   X. Xiao, T. E. Beechem, M. T. Brumbach, T. N. Lambert, D. J. Davis, J. R. Michael, C. M. Washburn, J. Wang, S. M. Brozik, D. R. Wheeler, D. B. Burckel and R. Polsky, *Acs Nano*, 2012, **6**, 3573.
10. R. Infuehr, N. Pucher, C. Heller, H. Lichtenegger, R. Liska, V. Schmidt, L. Kuna, A. Haase and J. Stampfl, *Appl. Surf. Sci.*, 2007, **254**, 836.